AD NUMBER

AD861437

LIMITATION CHANGES

TO:

Approved for public release; distribution is unlimited.

FROM:

**Distribution authorized to U.S. Gov't. agencies and their contractors;
Administrative/Operational Use; NOV 1969. Other requests shall be referred to Air Force Flight Dynamics Lab., Wright-Patterson AFB, OH 45433.**

AUTHORITY

AFWAL ltr dtd 6 Nov 1980

AERODYNAMIC CHARACTERISTICS OF BALLUTES AND DISK-GAP-BAND PARACHUTES AT MACH NUMBERS FROM 1.8 TO 3.7

Lawrence L. Galigher

ARO, Inc.

November 1969

PROPULSION WIND TUNNEL FACILITY
ARNOLD ENGINEERING DEVELOPMENT CENTER
AIR FORCE SYSTEMS COMMAND
ARNOLD AIR FORCE STATION, TENNESSEE

NOTICES

When U. S. Government drawings specifications, or other data are used for any purpose other than a definitely related Government procurement operation, the Government thereby incurs no responsibility nor any obligation whatsoever, and the fact that the Government may have formulated, furnished, or in any way supplied the said drawings, specifications, or other data, is not to be regarded by implication or otherwise, or in any manner licensing the holder or any other person or corporation, or conveying any rights or permission to manufacture, use, or sell any patented invention that may in any way be related thereto.

Qualified users may obtain copies of this report from the Defense Documentation Center.

References to named commercial products in this report are not to be considered in any sense as an endorsement of the product by the United States Air Force or the Government.

AERODYNAMIC CHARACTERISTICS OF BALLUTES AND DISK-GAP-BAND PARACHUTES AT MACH NUMBERS FROM 1.8 TO 3.7

Lawrence L. Galigher
ARO, Inc.

FOREWORD

The work reported herein was done at the request of the Air Force Flight Dynamics Laboratory (AFFDL), Air Force Systems Command (AFSC), and the National Aeronautics and Space Administration (NASA), Langley Research Center, under Program Element 62201F, Project 6065.

The results of tests presented were obtained by ARO, Inc. (a subsidiary of Sverdrup & Parcel and Associates, Inc.), contract operator of Arnold Engineering Development Center (AEDC), AFSC, Arnold Air Force Station, Tennessee, under Contract F40600-69-C-0001. The test was conducted from July 30 to September 13, 1969, under ARO Project Number PS0995; and the manuscript was submitted for publication on October 3, 1969.

This technical report has been reviewed and is approved.

George F. Garey
Major, USAF
Acting AF Representative, PWT
Directorate of Test

Roy R. Croy, Jr.
Colonel, USAF
Director of Test

ABSTRACT

A test was conducted in Propulsion Wind Tunnel, Supersonic (16S) to determine deployment characteristics and aerodynamic performance of disk-gap-band parachutes of various geometric porosities and ballutes with various ram-air inlet configurations. Deployments were made from a reentry-type model at nominal free-stream Mach numbers from 2.0 to 3.7 at a nominal free-stream dynamic pressure of 70 psf. Eight of the twelve parachutes tested failed shortly after data acquisition at the deployment Mach number test conditions. The six ballutes tested retained their structural integrity throughout the range of Mach numbers investigated.

CONTENTS

APPENDIXES

I. ILLUSTRATIONS

Figure

NOMENCLATURE

$A_{R/S}$	Ratio of projected, reefed canopy area to parachute canopy area
C_{D_o}	Average drag coefficient of decelerator plus model based either on parachute canopy area or on ballute inflated area, drag force/$q_\infty S$
$C_{D_{oi}}$	Mean decelerator-plus-model drag coefficient value of each cell in the statistical analysis program, drag force/$q_\infty S$
M_∞	Free-stream Mach number
N	Total number of drag coefficient data samples used in the statistical analysis program
N_i	Number of drag coefficient data samples in each cell of the statistical analysis program
$(Ni)_{max}$	Maximum number of drag coefficient data samples in any cell of the statistical analysis program

q_∞	Free-stream dynamic pressure, psf
S	Total area of a drag-producing surface, which includes all openings in the drag-producing surface, such as slots and vent for parachutes and frontal projected area for ballutes; S = 23.758 ft^2 (parachute), S = 12.566 ft^2 (4-ft-diam ballute), and S = 1.227 ft^2 (15-in.-diam ballute)
x/D	Decelerator separation distance from forebody expressed in forebody base diameters
$\sqrt{\beta_1}$	Skewness parameter of a distribution of drag coefficient data determined from the statistical analysis program
β_2	Kurtosis parameter of a distribution of drag coefficient data determined from the statistical analysis program
σ	Standard deviation of a distribution of drag coefficient data determined from the statistical analysis program
λ	Ratio of the open area of a canopy drag-producing surface to the total canopy drag-producing surface area
Relative Dynamic Parameter	Ratio of the 95-percent confidence level interval, expressed as drag coefficient interval, of a distribution of drag coefficient data to the average drag coefficient value as determined from the statistical analysis program

SECTION I
INTRODUCTION

Supersonic aerodynamic decelerators are scheduled for rocket-powered free-flight and captive sled development tests by the National Aeronautics and Space Administration (NASA), Langley Research Center, and the Air Force Flight Dynamics Laboratory (AFFDL), respectively, to determine optimum decelerator configurations for specific decelerator system application. Prior knowledge of the effect of various decelerator design parameters on the performance characteristics of various decelerator types would provide the data necessary to limit the selection of decelerators to be investigated in free-flight and captive sled development tests. The effect of various design parameters on the performance characteristics of three types of decelerators were investigated in a three-phase test program conducted in Propulsion Wind Tunnel, Supersonic (16S) at Mach numbers from 2.0 to 4.75. The results of the first and second phase of testing are reported in Refs. 1 and 2. The purpose of the first and second phases of testing was to determine deployment characteristics and aerodynamic performance of Supersonic X parachutes and attached inflatable decelerators, respectively. The purpose of the third phase of testing, reported herein, was to determine deployment characteristics and aerodynamic performance of ballutes and disk-gap-band (DGB) parachutes (10-, 12.5- and 15-percent porosity). These decelerators were deployed from a reentry-type model at Mach numbers from 2.0 to 3.7 at a free-stream dynamic pressure of 70 psf. Twelve parachutes and six ballutes were deployed during this phase of testing.

SECTION II
APPARATUS

2.1 TEST FACILITY

Tunnel 16S is a closed-circuit, continuous-flow wind tunnel that presently can be operated at Mach numbers from 1.50 to 4.75. The tunnel can be operated over a stagnation pressure range from 200 psfa to a maximum of 2300 psfa. The maximum stagnation temperature varies from 300°F at Mach number 1.5 to 620°F at Mach number 3.0. The minimum stagnation temperature varies from 100 to 120°F. The tunnel specific humidity is controlled by removing tunnel air and supplying conditioned makeup air from an atmospheric dryer.

Details of the test section showing the model location and strut support arrangement are shown in Fig. 1, Appendix I. A more extensive description of the tunnel and its operating characteristics is contained in Ref. 3.

2.2 TEST ARTICLES

The model consisted of a reentry-type body with provisions for attachment of conical aeroshells having base diameters of 12 and 19 in. The model was attached to a cone-cylinder forebody through a two-degree-of-freedom (pitch and yaw) universal joint. The forebody, in turn, was attached to the strut support arrangement through an internally-mounted load cell. Major model details and dimensions are presented in Fig. 2, and wind tunnel installation photographs of the model with and without the conical aeroshells are presented in Fig. 3. A photograph of the model with a stowed decelerator is shown in Fig. 4.

The decelerator package was restrained against a spring-loaded base plate by a series of straps that were tied together by a restraining cord as shown previously in Fig. 4. A pyrotechnic cutter was used to sever the restraining cord. Several parachute packages contained an additional line cutter that severed a canopy reefing line 3 to 10 sec after initiation of the deployment sequence.

Major details and dimensions of the DGB parachutes and the ballutes are shown in Figs. 5 and 6, respectively. The parachutes were constructed of Dacron® cloth (2.25 oz/yd^2), and the ballutes were constructed of Dacron cloth (4.35 oz/yd^2) coated with 1473-C Neoprene®. The inflated parachute diameter was 4 ft, and the leading edge of the canopy was located 6.8 ft aft of the model base. Parachute geometric porosities of 10-, 12.5- and 15-percent were obtained by varying the band- and air-gap dimensions as tabulated in Fig. 5. The inflated diameter of the ballute was 4 ft, and the apex of the ballute constructed with peripheral ram-air inlets was located 3.5 ft aft of the model base. The apex of the ballute constructed with both an apex ram-air inlet and peripheral ram-air inlets was located 3.78 ft aft of the model base. In addition to tests of the 4-ft-diam ballutes, a 15-in.-diam ballute with four peripheral ram-air inlets was also tested. The apex of this ballute was located 6.3 ft aft of the model base. All decelerator riser lines were attached to the model through a swivel-tensiometer-bridle arrangement.

2.3 INSTRUMENTATION

A 2000-lb capacity load cell and a 1800-lb capacity tensiometer were used to measure forebody-plus-model-plus-decelerator drag and decelerator drag, respectively, within an accuracy of ±10 lb. Four motion-picture cameras and two television cameras, installed in the test section walls, were used to document and monitor the test.

The outputs from the load cell and tensiometer were digitized and permanently recorded on magnetic tape for on-line data reduction, and the load cell output was recorded on a high-speed digital data recording system at a sampling rate of 1000 samples per second for off-line data reduction. These outputs were also continuously recorded on direct-writing and film pack oscillographs for monitoring model dynamics.

SECTION III
PROCEDURE

The decelerator package was attached to the model before wind tunnel test operation was initiated. Once the prescribed test conditions were established, steady-state data were obtained for the undeployed configuration. A countdown procedure was used to sequence data acquisition during decelerator deployment. The deployment procedure consisted of activating the recording oscillographs, test section cameras, and the high-speed digital data recording system, followed by severing the decelerator restraining cord with a pyrotechnic cutter. Upon completion of the decelerator deployment sequence, steady-state drag loads were calculated by averaging the analog outputs from the load cell and tensiometer over 1-sec intervals. Drag distribution parameters, such as average drag coefficient, standard deviation, skewness and kurtosis, were calculated from the data recorded on the high-speed digital data recording system from a statistical analysis program (Appendix II).

Twelve DGB parachutes of various geometric porosities, five 4-ft-diam ballutes of various ram-air inlet configurations, and a 15-in.-diam ballute were tested through the Mach number range from 1.8 to 3.7 at a nominal free-stream dynamic pressure of 70 psf. The decelerators were deployed at various Mach numbers; and, after data acquisition was completed, the decelerator performance was investigated at other Mach numbers. However, eight of the twelve parachutes tested failed shortly after data acquisition at the deployment test condition. A summary of the test conditions established for each decelerator is presented in Table I (Appendix III).

SECTION IV
RESULTS AND DISCUSSION

Only the data obtained from the load cell, which measured decelerator-plus-forebody loads, are presented in this report because the tensiometer malfunctioned during a considerable portion of the test program. Data are presented for the model with a stowed decelerator package throughout the Mach number test range.

4.1 DECELERATOR DYNAMIC CHARACTERISTICS

Drag time-history traces of a reefed parachute deployment, an unreefed parachute deployment, and a ballute deployment are presented in Fig. 7. These data show that the parachute drag dynamics were less severe in the reefed configuration than in the unreefed configuration. The ballute drag dynamics were negligible once the ballute attained full inflation.

The motion-picture films show that the canopies of all unreefed parachutes were fully inflated throughout the Mach number range of the test. Six of the twelve parachutes tested were deployed in the reefed configuration, of which three were disreefed 3 sec after deployment and one was disreefed 10 sec after deployment. In general, the parachutes in the reefed configuration exhibited less motion than the parachutes in the unreefed configuration. One of the two permanently reefed parachutes (Config. 20), which was tested with a reefed area ratio of 0.081, exhibited sporadic pulsing of the canopy through the Mach number range from 2.0 to 2.5. The motion of the unreefed parachutes increased slightly as Mach number was increased; and, at a given Mach number, the motion of the parachute was less with an aeroshell attached to the model than without an aeroshell. There was no discernible effect of geometric porosity on the motion of the parachute. All of the ballutes tested except one attained full inflation and exhibited essentially no motion. The failure of one of the ballutes to attain full inflation was attributed to the use of an apex ram-air inlet instead of peripheral ram-air inlets.

The dynamic drag characteristics of each decelerator, at the deployment Mach number only, were determined from a statistical analysis program (Appendix II). The statistical program reduces the data recorded by a high-speed digital data recording system at a sample rate of 1000 samples per second and calculates drag distribution parameters, average drag coefficient, standard deviation, skewness,

and kurtosis. The drag distribution parameters are tabulated on the dynamic drag coefficient distribution plots presented in Fig. 8. Also shown on each plot is the 95-percent confidence level interval determined from the drag distribution parameters. This interval can be interpreted as representing a quantitative measurement of decelerator drag dynamics at a 95-percent confidence level. To compare drag dynamics of one decelerator with those of another decelerator, it is first necessary to divide the 95-percent confidence level interval, expressed as drag coefficient interval, by the average drag coefficient to obtain a relative drag dynamic level for each decelerator. This term will be referred to as the relative dynamic parameter, and its value is tabulated in Table I for each decelerator. The significance of the relative dynamic parameter can be discerned by explaining the drag dynamics characteristics of a decelerator when values of zero, unity, and two are assigned to the relative dynamic parameter. A value of zero implies no dynamics, a value of unity implies that the magnitude of dynamics about the average drag coefficient value is equal to 50 percent of the average drag coefficient, and a value of two implies that the magnitude of dynamics about the average drag coefficient value is equal to 100 percent of the average drag coefficient.

The variation of the relative dynamic parameter with parachute porosity and free-stream Mach number is shown in Figs. 9 and 10, respectively. These data indicate that the parachute dynamics increased for the higher Mach numbers and that, at $M_\infty = 3.0$, the parachute dynamics were less with an attached aeroshell than without an aeroshell. Data for the two permanently reefed parachutes indicate that drag dynamics decreased approximately 51 and 81 percent for reefed area ratios of 0.153 and 0.081, respectively. Parachute porosity had no effect on drag dynamics at $M_\infty = 2.0$; but at $M_\infty = 2.5$, the drag dynamics decreased slightly for the higher porosity parachute. The ballute data indicate negligible drag dynamics. The results obtained from analysis of the relative dynamic parameter are in good agreement with the results obtained from the motion-picture films.

4.2 DECELERATOR STEADY-STATE PERFORMANCE

The variation of parachute-plus-forebody drag coefficient with Mach number is shown in Fig. 11. At a given Mach number, the parachute-plus-forebody drag coefficients obtained with and without an attached aeroshell were of equal magnitude because of forebody wake effects. In the Mach number range from 2.0 to 2.5, canopy reefing resulted in drag reductions of approximately 52 and 64 percent for parachutes with reefed area ratios of 0.153 and 0.081, respectively. The

data presented in Fig. 12 show that a 50-percent increase in parachute geometric porosity resulted in a drag reduction of approximately 6 percent at $M_\infty = 2.0$. The limited amount of data obtained at $M_\infty = 2.5$ indicate that parachute drag coefficient was invariant with geometric porosity.

Five ballutes with various ram-air inlet configurations were tested in the Mach number range from 2.0 to 3.7. The data presented in Fig. 13 show that four of the five ram-air inlet configurations tested had no effect on the magnitude of the ballute drag coefficient. The exception was a ballute with a single apex ram-air inlet that failed to inflate and, subsequently, resulted in a drag reduction of approximately 78 percent at the deployment Mach number of 3.7. Except for the ballute that failed to inflate, the inflation time decreased as the number of ram-air inlets was increased. The data presented in Fig. 14 show that inflation time decreased approximately 22 percent as the number of ram-air inlets was increased from two to five.

The data obtained from tests of the 15-in.-diam ballute are presented in Fig. 15. These data indicate that, at $M_\infty = 3.68$, the drag of the 19-in.-diam aeroshell was approximately 50 percent of the total drag of the deployed ballute plus forebody. Forebody drag data were only obtained at $M_\infty = 3.68$.

SECTION V
CONCLUDING REMARKS

Tests were conducted to determine deployment characteristics and aerodynamic performance of DGB parachutes of various geometric porosities and ballutes with various ram-air inlet configurations. Deployments were made from a reentry-type model at nominal free-stream Mach numbers from 2.0 to 3.7 at a nominal free-stream dynamic pressure of 70 psf. The following observations are a result of these tests:

1. Eight of the twelve parachutes tested failed shortly after data acquisition at the deployment Mach number test condition.
2. The parachute drag dynamics increased as Mach number was increased; and, at $M_\infty = 3.0$, the parachutes exhibited less drag dynamics with a 12-in. aeroshell attached to the forebody than without an attached aeroshell.

3. Drag dynamics decreased approximately 51 and 81 percent for parachutes with reefed area ratios of 0.153 and 0.081, respectively.
4. At Mach numbers from 2.0 to 2.5, parachute canopy reefing resulted in drag reductions of approximately 52 and 64 percent for parachutes with reefed area ratios of 0.153 and 0.081 respectively.
5. At M_∞ = 2.0, a 50-percent increase in parachute geometric porosity resulted in a drag reduction of approximately 6 percent.
6. Four of the five ram-air inlet ballute configurations tested attained full inflation, and ballute inlet configuration had no effect on the magnitude of the ballute drag coefficient.
7. Ballute inflation time decreased approximately 22 percent as the number of ram-air inlets was increased from two to five.

REFERENCES

1. Galigher, Lawrence L. "Aerodynamic Characteristics of Supersonic X Parachutes at Mach Numbers of 2.1 and 4.0." AEDC-TR-69-8 (AD846695), January 1969.
2. Baker, D. C. "Investigation of an Attached Inflatable Decelerator with Mechanically Deployed Inlets at Mach Numbers from 2.25 to 4.75." AEDC-TR-69-132 (AD854437), June 1969.
3. Test Facilities Handbook (7th Edition). "Propulsion Wind Tunnel Facility, Vol. 5." Arnold Engineering Development Center, July 1968.
4. Hahn, Gerald J. and Shapiro, Samuel S. Statistical Models in Engineering. John Wiley and Sons, Inc., New York, 1967.

APPENDIXES

I. ILLUSTRATIONS
II. STATISTICAL ANALYSIS PROGRAM
III. TABLE

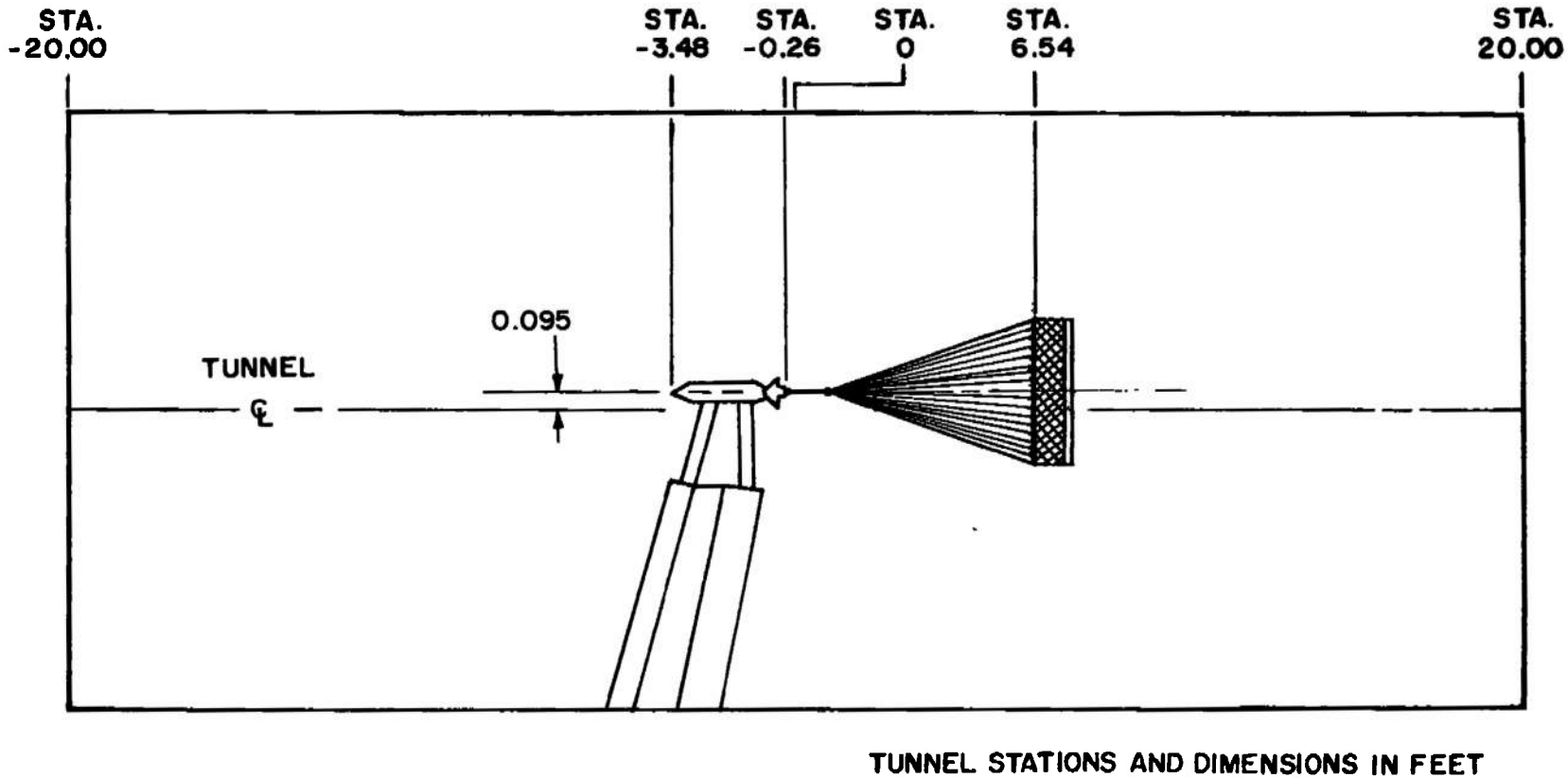

Fig. 1 Model Location in Test Section

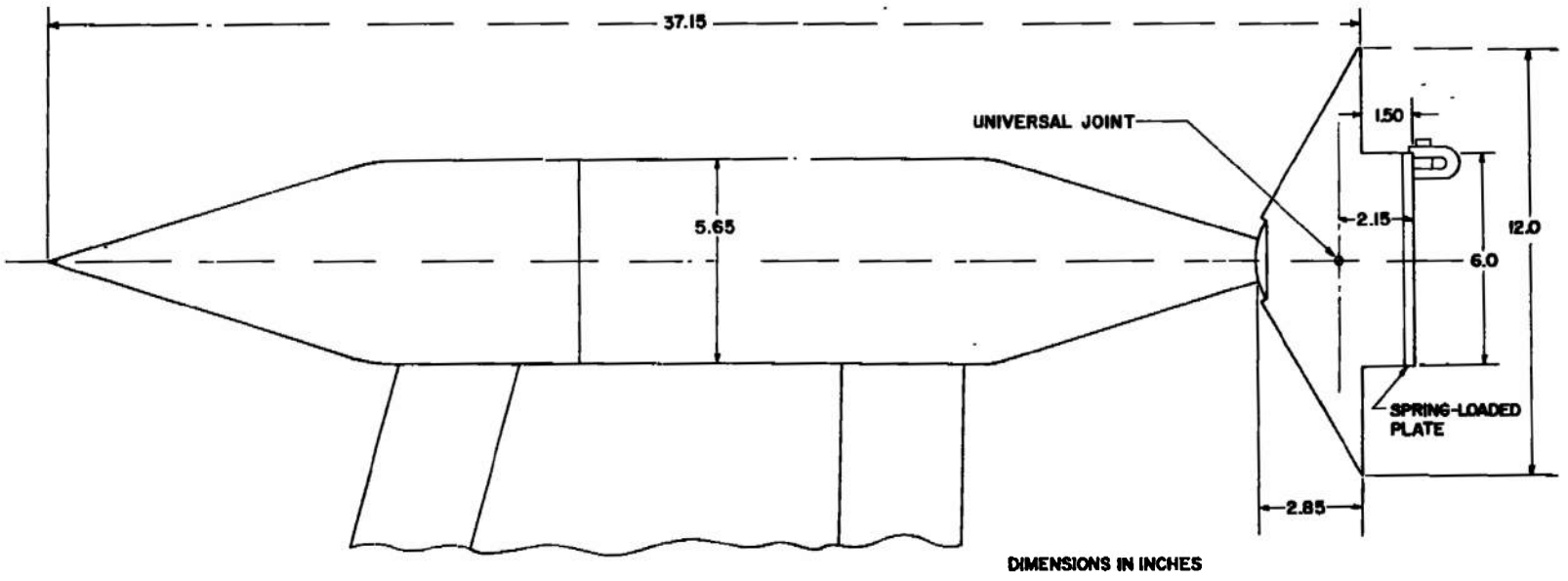

Fig. 2 Dimensioned Sketch of Test Article

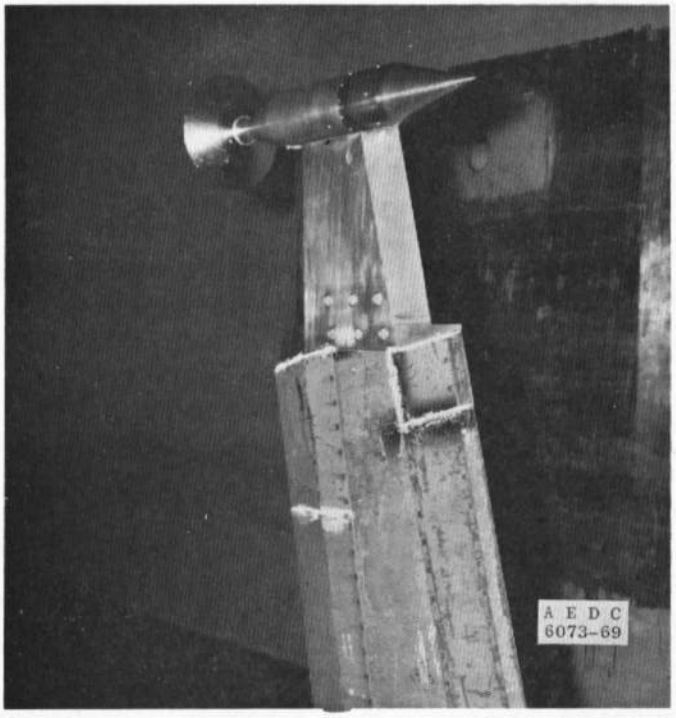

a. Model with Attoched 12-in.-Diam Aeroshell

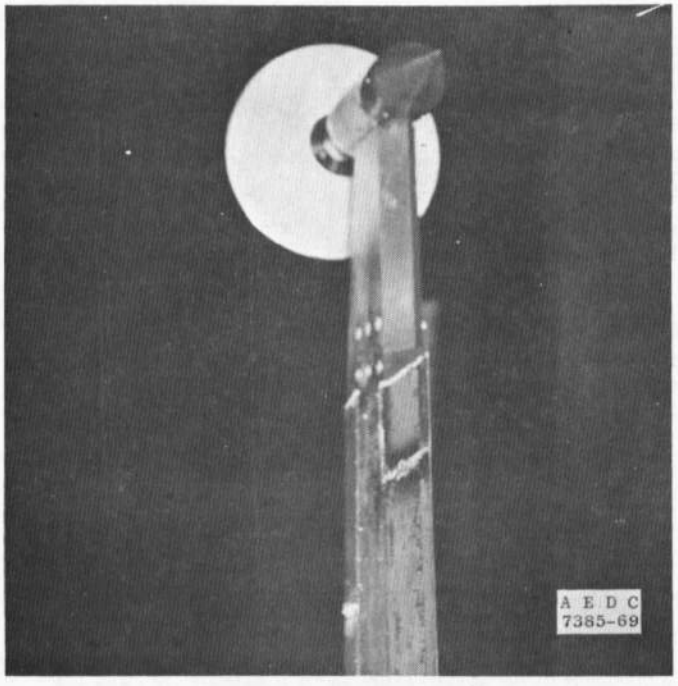

b. Model with Attached 19-in.-Diam Aeroshell

Fig. 3 Model Installation in Test Section

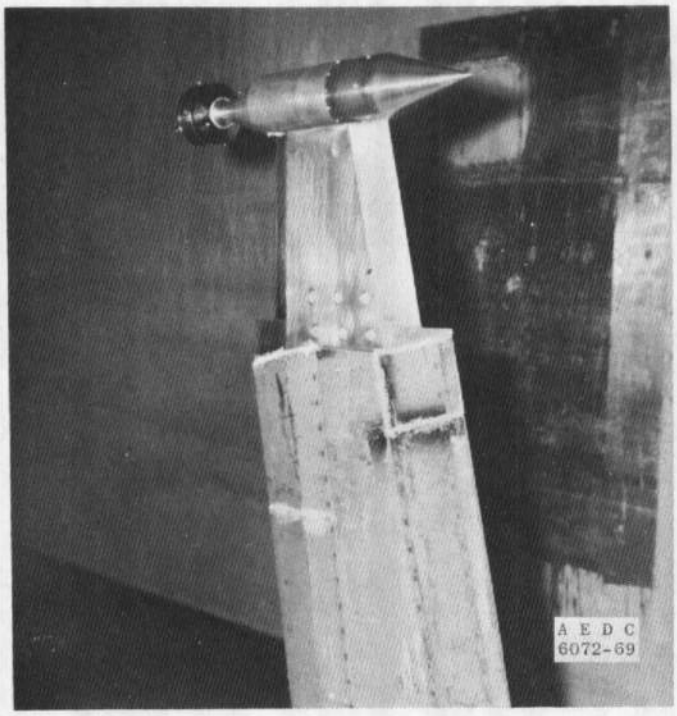

c. Model without on Attached Aeroshell

Fig. 3 Concluded

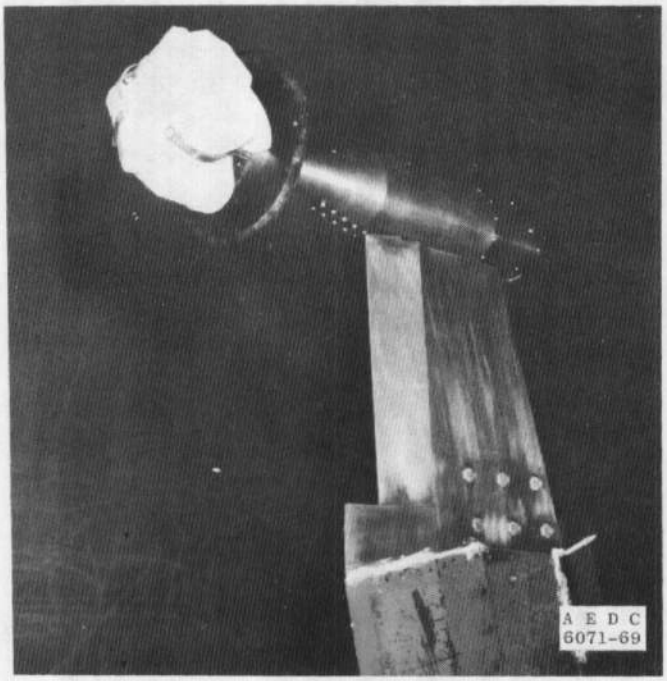

Fig. 4 Model with Stowed Decelerator Package

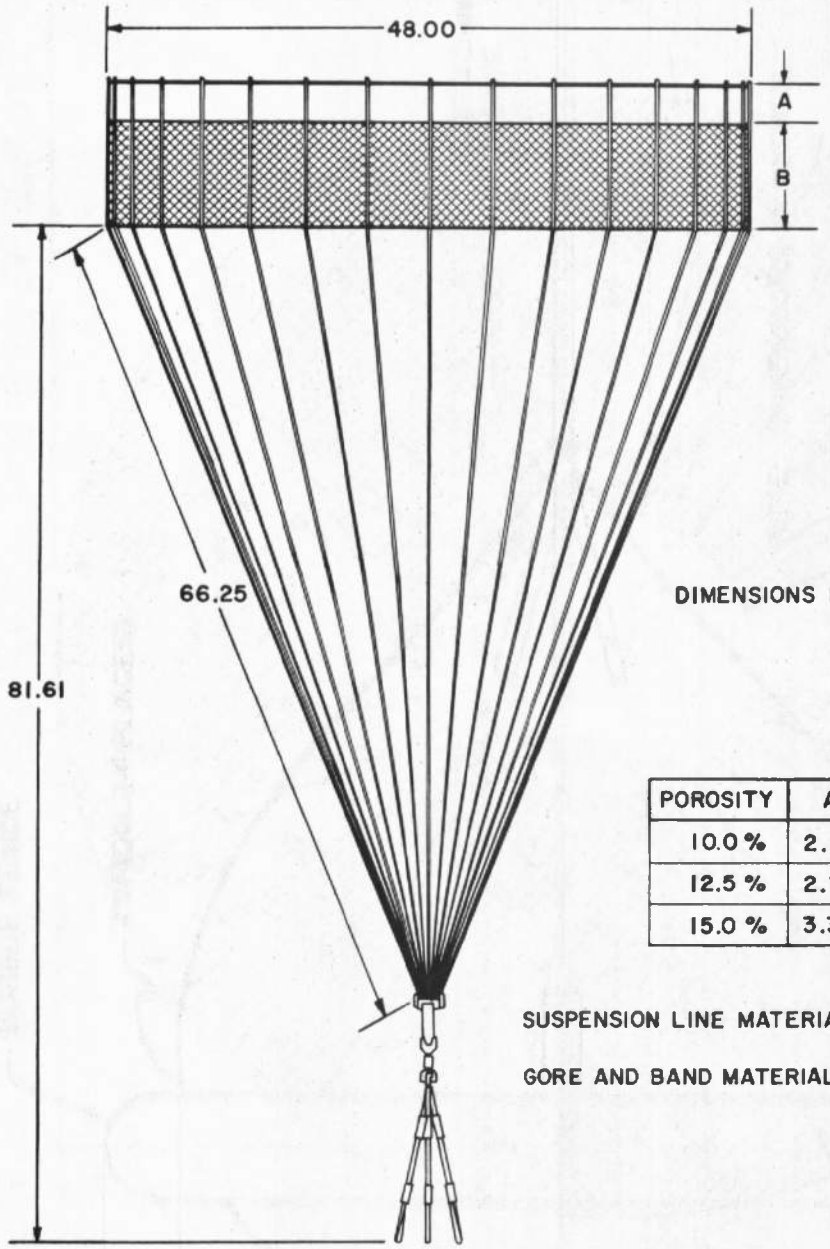

DIMENSIONS IN INCHES

POROSITY	A	B
10.0 %	2.18	8.47
12.5 %	2.75	7.90
15.0 %	3.32	7.33

SUSPENSION LINE MATERIAL: DACRON CORD, 300lb TENSILE STRENGTH

GORE AND BAND MATERIAL: DACRON CLOTH, 2.25 oz/yd^2

a. Profile

Fig. 5 Disk-Gap-Band Parachute Details

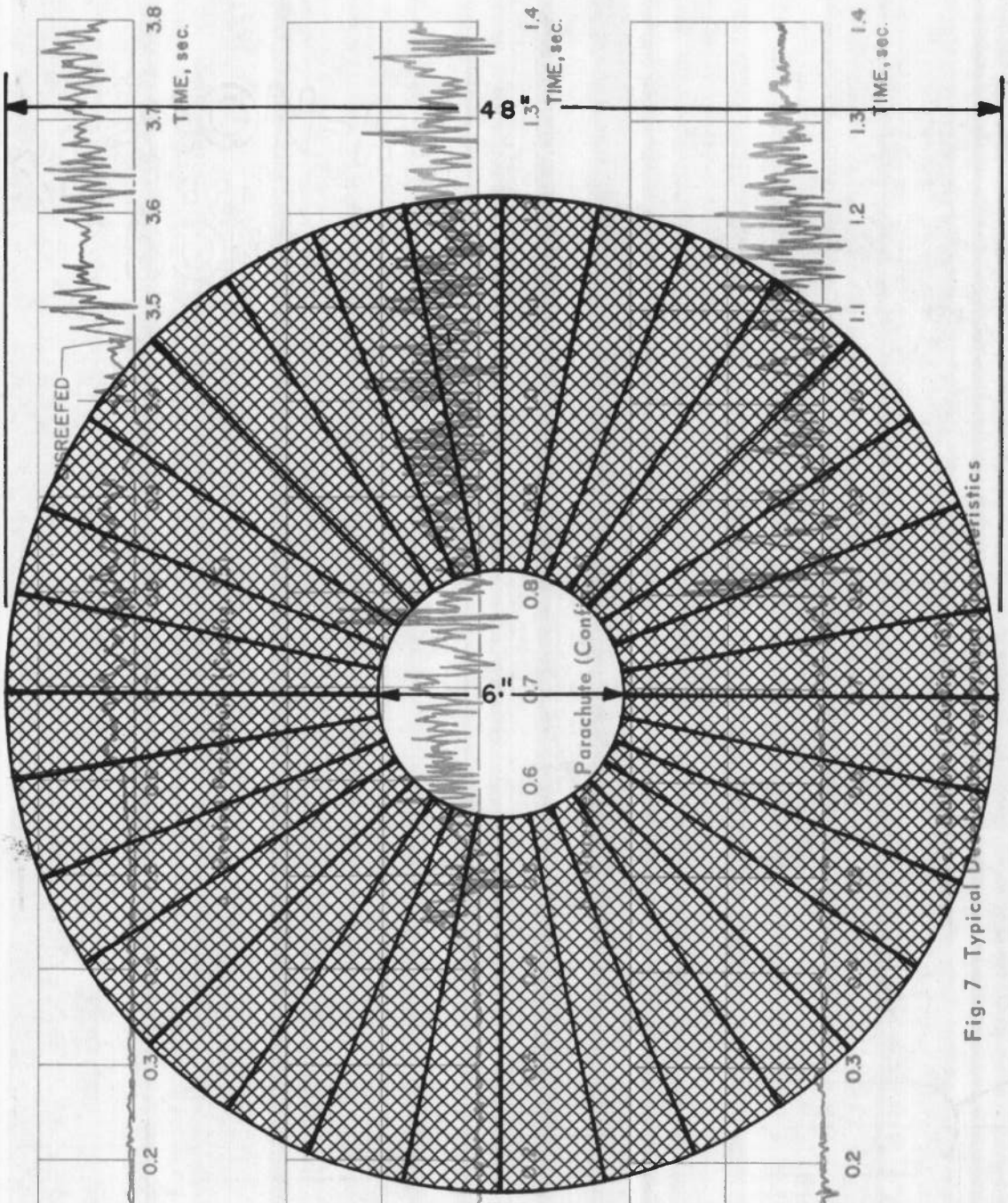

GORE AND BAND MATERIAL: DACRON CLOTH, 2.25 oz/yd

b. Roof

Fig. 5 Concluded

Fig. 7 Typical D... Characteristics

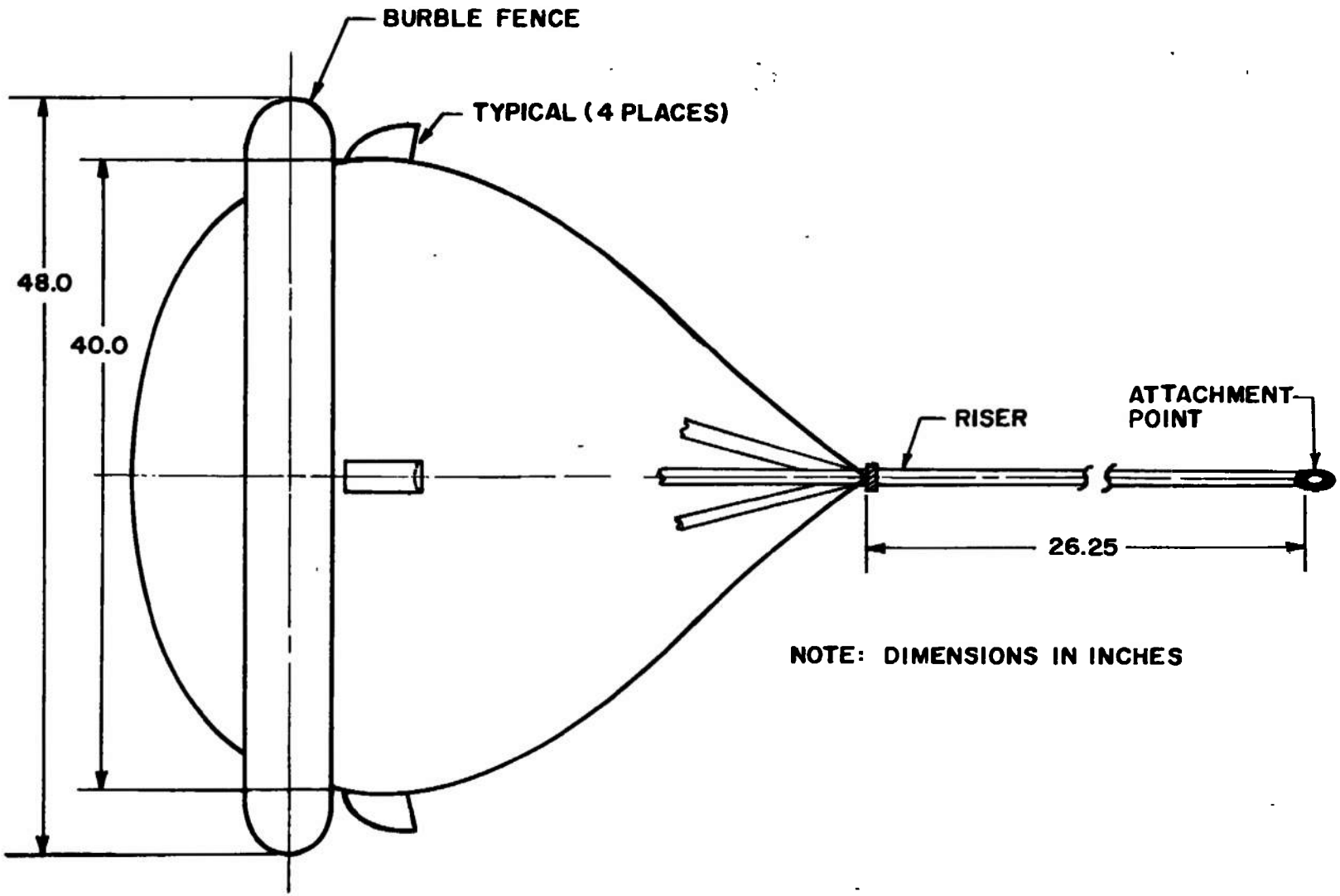

Fig. 6 Ballute Details

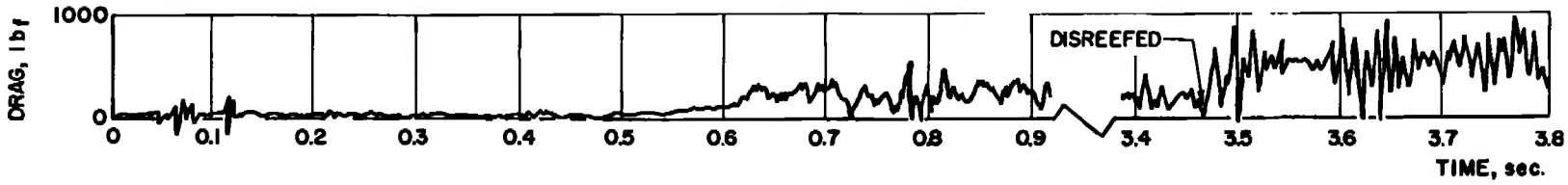

a. Reefed Parachute (Config. 15)

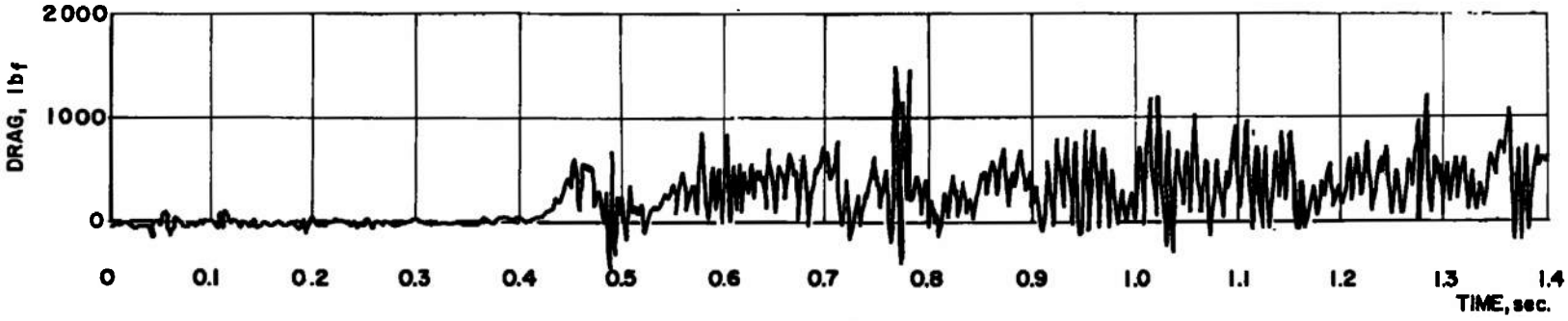

b. Unreefed Parachute (Config. 6)

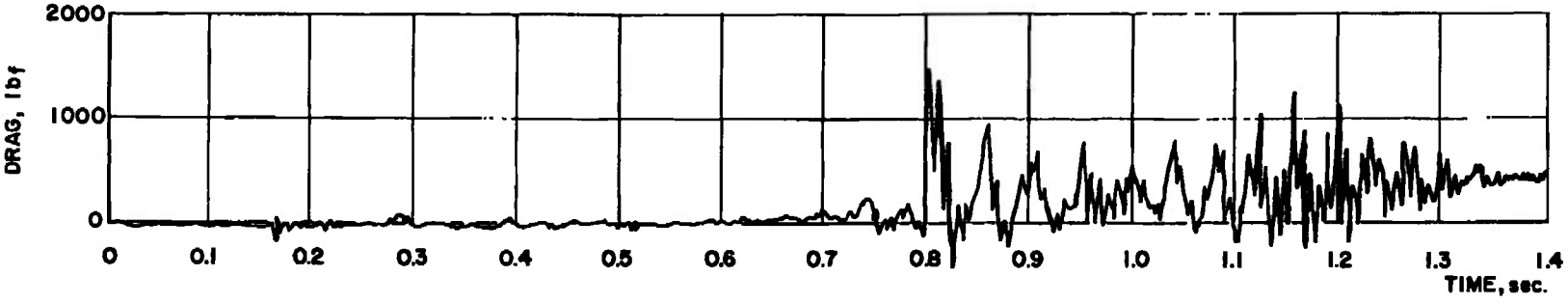

c. Ballute (Config. 13)

Fig. 7 Typical Decelerator Deployment Characteristics

C_{D_0}	σ	SKEWNESS	KURTOSIS	$(N_i)_{MAX}$	N
0.3810	0.1518	0.1040	2.8618	422	12770

$C_{D_0} = 0.3810 \quad {}^{+0.3057}_{-0.2875}$ (95% CONFIDENCE LEVEL)

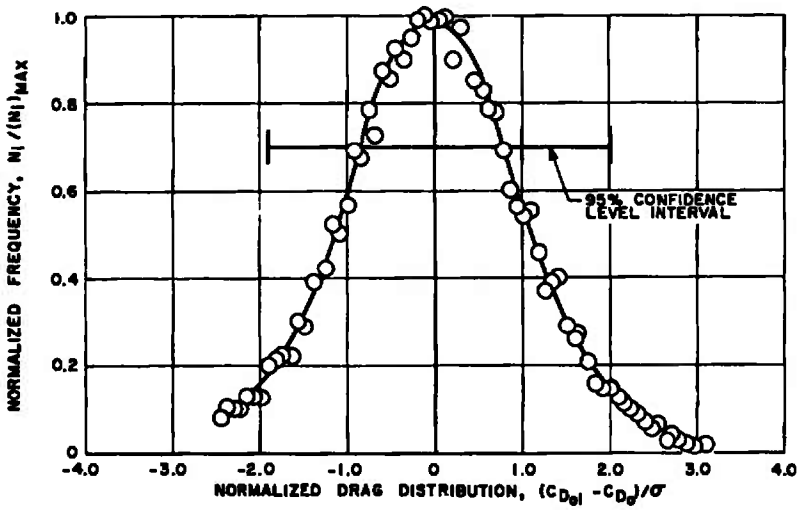

a. DGB 10-percent Porosity Parachute (Config. 8), $M_\infty = 2.0$

C_{D_0}	σ	SKEWNESS	KURTOSIS	$(N_i)_{MAX}$	N
0.2931	0.1328	0.2807	2.8301	514	15587

$C_{D_0} = 0.2931 \quad {}^{+0.2753}_{-0.2377}$ (95% CONFIDENCE LEVEL)

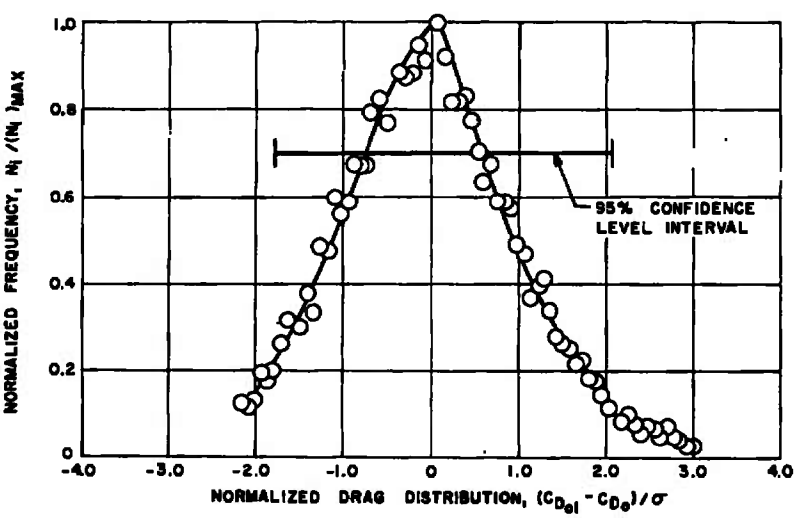

b. DGB 10-percent Porosity Parachute (Config. 10), $M_\infty = 2.5$

Fig. 8 Distribution Plots of Decelerator Dynamic Drag Characteristics

C_{D_0}	σ	SKEWNESS	KURTOSIS	$(N_i)_{MAX}$	N
0.3670	0.1485	0.2321	3.2963	748	16941

$C_{D_0} = 0.3670 \; {}^{+0.3079}_{-0.2771}$ (95% CONFIDENCE LEVEL)

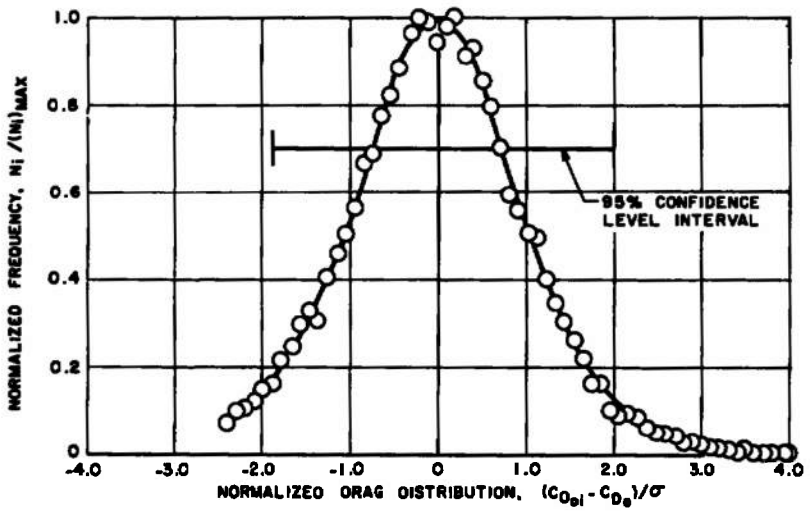

c. DGB 12.5-percent Porosity Parachute (Config. 7), $M_\infty = 2.0$

C_{D_0}	σ	SKEWNESS	KURTOSIS	$(N_i)_{MAX}$	N
0.3636	0.1038	-0.0729	3.2524	820	15976

$C_{D_0} = 0.3636 \; {}^{+0.2025}_{-0.2073}$ (95% CONFIDENCE LEVEL)

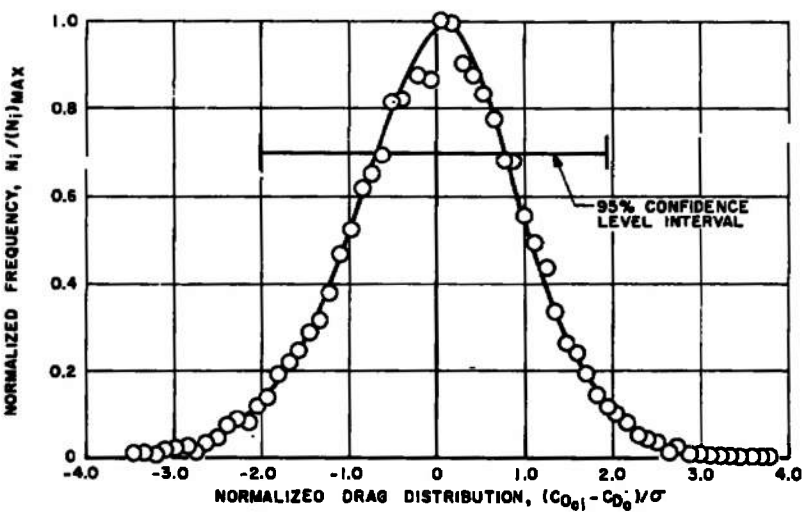

d. DGB 12.5-percent Porosity Parachute (Config. 15), $M_\infty = 2.0$

Fig. 8 Continued

C_{D_0}	σ	SKEWNESS	KURTOSIS	$(N_i)_{MAX}$	N
0.2383	0.1374	0.5944	3.1167	491	15041

$C_{D_0} = 0.2383 \; {}^{+0.3065}_{-0.2185}$ (95% CONFIDENCE LEVEL)

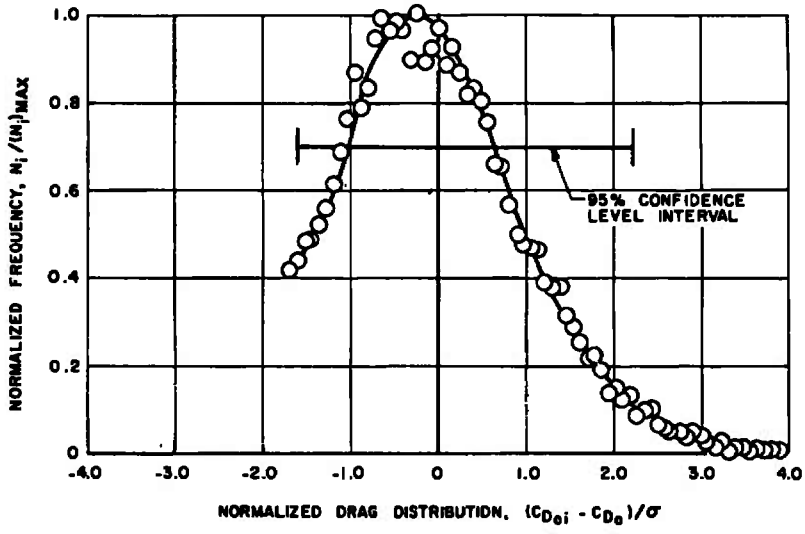

e. DGB 12.5-percent Porosity Parachute (Config. 6), M_∞ = 3.0

C_{D_0}	σ	SKEWNESS	KURTOSIS	$(N_i)_{MAX}$	N
0.3691	0.1535	0.1978	2.9871	552	12777

$C_{D_0} = 0.3691 \; {}^{+0.3147}_{-0.2847}$ (95% CONFIDENCE LEVEL)

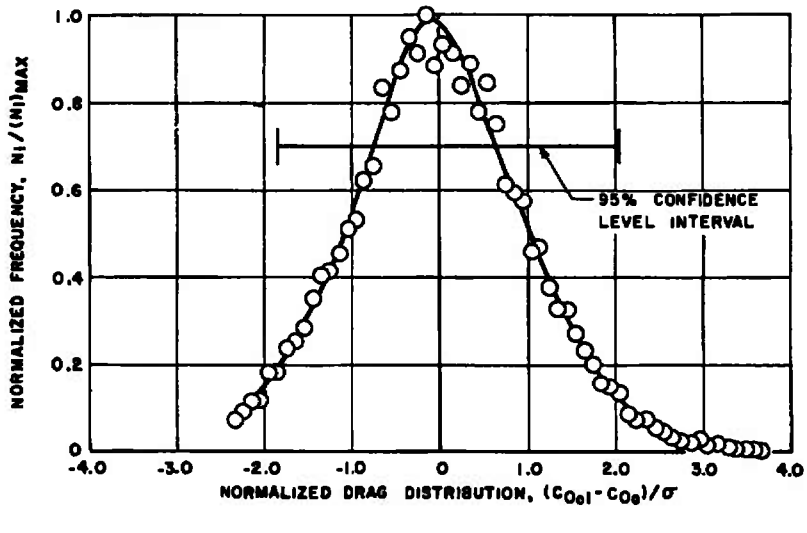

f. DGB 12.5-percent Porosity Parachute (Config. 3), M_∞ = 2.0

Fig. 8 Continued

C_{D_0}	σ	SKEWNESS	KURTOSIS	$(N_i)_{MAX}$	N
0.1534	0.0360	0.0708	3.4546	1600	16001

$C_{D_0} = 0.1534 \quad {}^{+0.0720}_{-0.0707}$ (95% CONFIDENCE LEVEL)

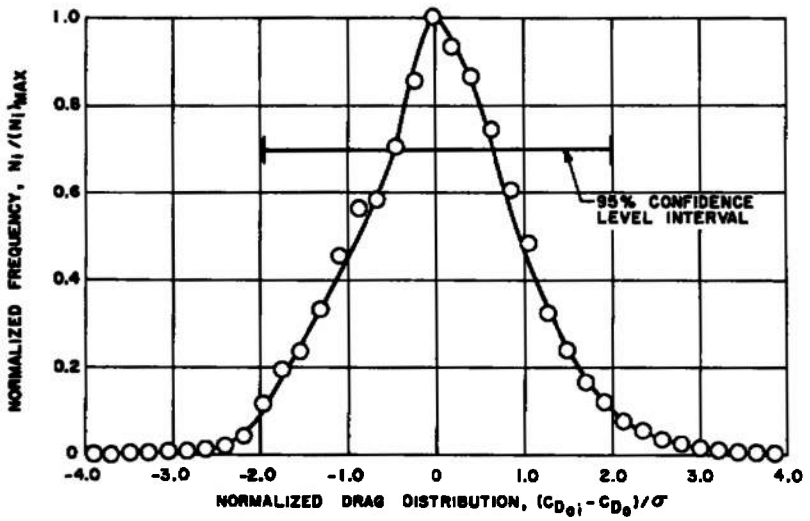

g. DGB 12.5-percent Porosity Parachute (Config. 19), $M_\infty = 2.5$

C_{D_0}	σ	SKEWNESS	KURTOSIS	$(N_i)_{MAX}$	N
0.0991	0.0083	0.0482	2.5826	2357	16001

$C_{D_0} = 0.0991 \quad {}^{+0.0160}_{-0.0158}$ (95% CONFIDENCE LEVEL)

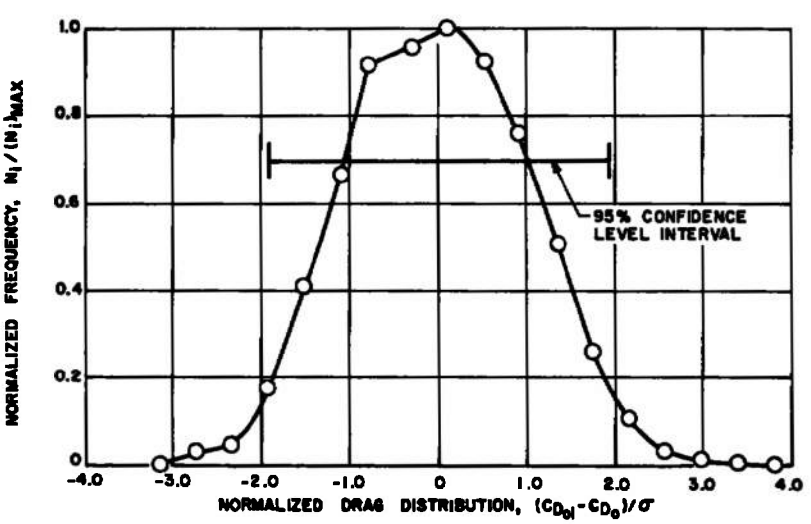

h. DGB 12.5-percent Porosity Parachute (Config. 20), $M_\infty = 2.5$

Fig. 8 Continued

C_{D_0}	σ	SKEWNESS	KURTOSIS	$(N_i)_{MAX}$	N
0.2482	0.1259	0.3953	3.0606	561	15540

$C_{D_0} = 0.2482 \; {}^{+0.2647}_{-0.2160}$ (95% CONFIDENCE LEVEL)

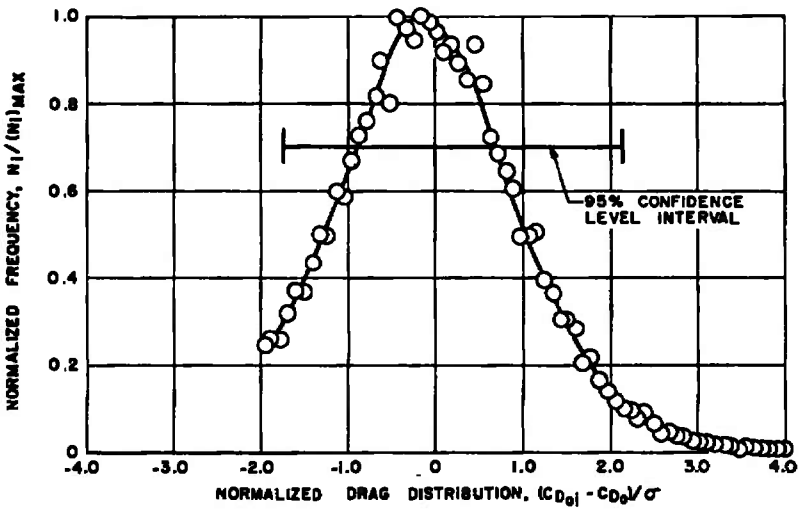

i. DGB 12.5-percent Porosity Parachute (Config. 1), $M_\infty = 3.0$

C_{D_0}	σ	SKEWNESS	KURTOSIS	$(N_i)_{MAX}$	N
0.2388	0.1091	0.3629	3.1408	676	15704

$C_{D_0} = 0.2388 \; {}^{+0.2318}_{-0.1940}$ (95% CONFIDENCE LEVEL)

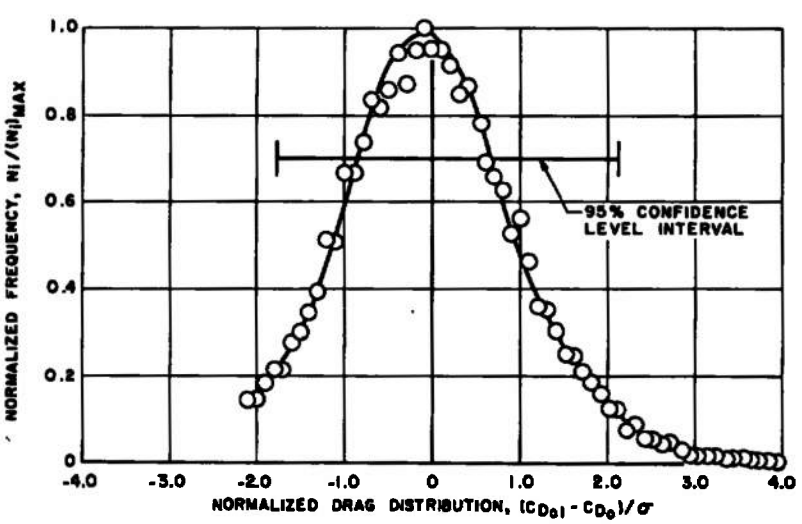

j. DGB 12.5-percent Porosity Parachute (Config. 2), $M_\infty = 3.0$

Fig. 8 Continued

C_{D_0}	σ	SKEWNESS	KURTOSIS	$(N_i)_{MAX}$	N
0.3587	0.1420	0.2185	3.1528	597	15746

$C_{D_0} = 0.3587 \; {}^{+0.2919}_{-0.2638}$ (95% CONFIDENCE LEVEL)

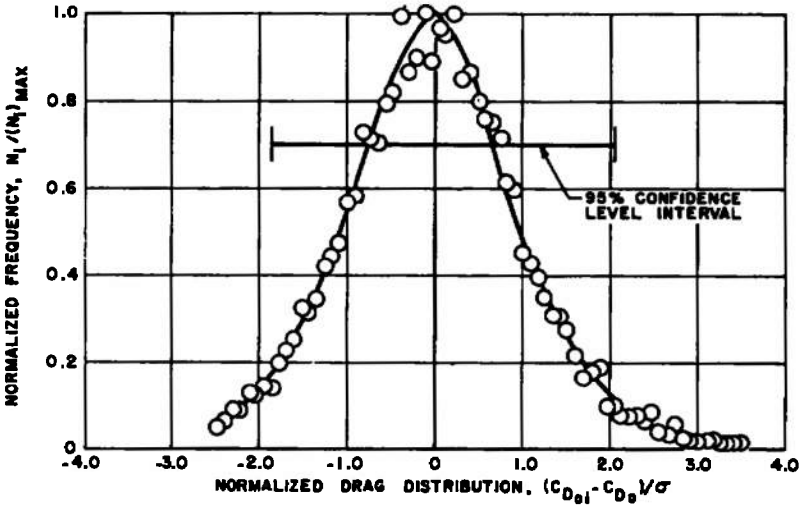

k. DGB 15-percent Porosity Parachute (Config. 9), $M_\infty = 2.0$

C_{D_0}	σ	SKEWNESS	KURTOSIS	$(N_i)_{MAX}$	N
0.2953	0.1252	0.3885	3.3691	755	15816

$C_{D_0} = 0.2953 \; {}^{+0.2679}_{-0.2237}$ (95% CONFIDENCE LEVEL)

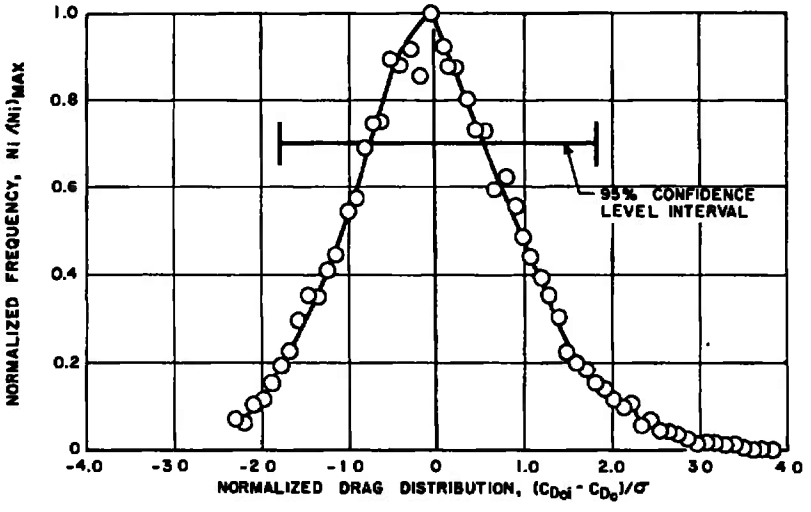

l. DGB 15-percent Porosity Parachute (Config. 11), $M_\infty = 2.5$

Fig. 8 Continued

C_{D_0}	σ	SKEWNESS	KURTOSIS	$(N_i)_{MAX}$	N
0.6218	0.0073	0.0294	2.4649	3380	16424

$C_{D_0} = 0.6128\ ^{+0.0141}_{-0.0135}$ (95% CONFIDENCE LEVEL)

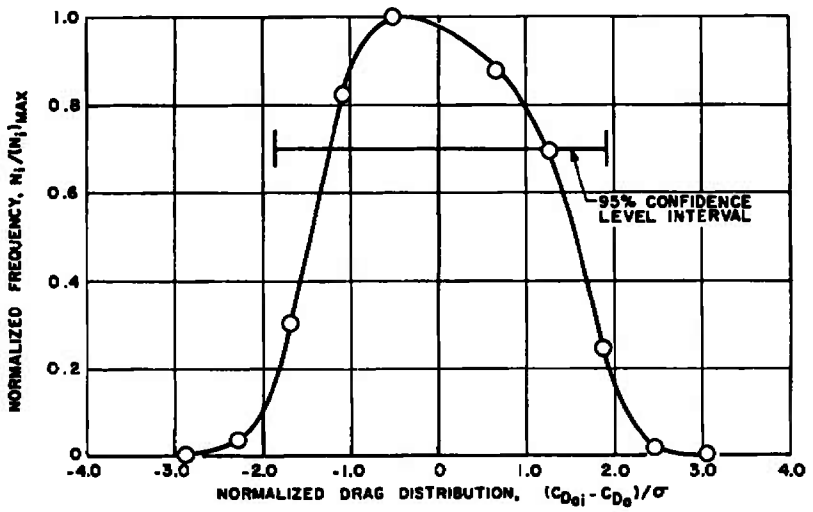

m. Ballute (Config. 13), $M_{\infty} = 3.69$

C_{D_0}	σ	SKEWNESS	KURTOSIS	$(N_i)_{MAX}$	N
0.6182	0.0134	0.0406	2.1723	1677	16001

$C_{D_0} = 0.6182\ ^{+0.0254}_{-0.0242}$ (95% CONFIDENCE LEVEL)

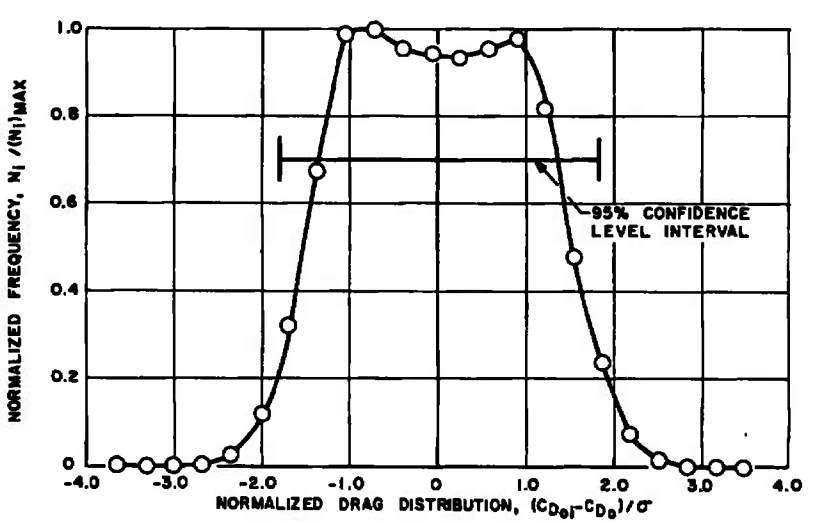

n. Ballute (Config. 4), $M_{\infty} = 3.68$

Fig. 8 Continued

C_{D_0}	σ	SKEWNESS	KURTOSIS	$(N_i)_{MAX}$	N
0.6168	0.0076	-0.0917	3.4958	2979	15925

$C_{D_0} = 0.6168 \; {}^{+0.0148}_{-0.0153}$ (95% CONFIDENCE LEVEL)

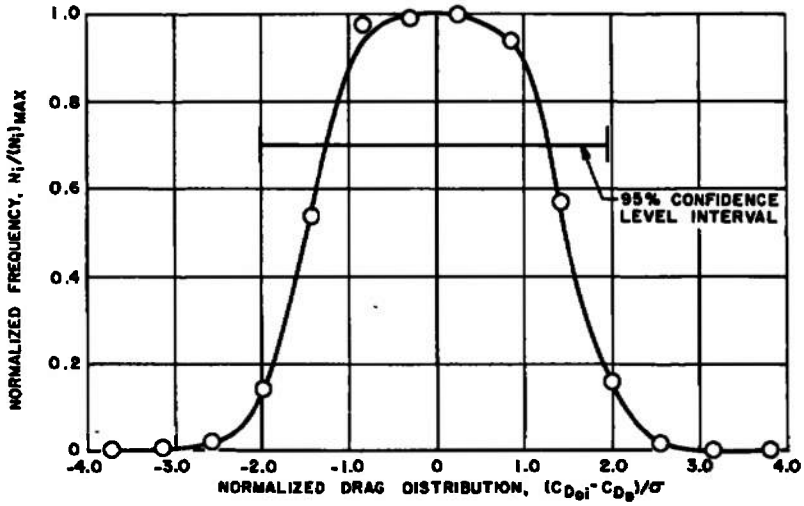

o. Ballute (Config. 12), $M_\infty = 3.69$

C_{D_0}	σ	SKEWNESS	KURTOSIS	$(N_i)_{MAX}$	N
0.6142	0.0073	0.0346	2.3548	3170	16001

$C_{D_0} = 0.6142 \; {}^{+0.0136}_{-0.0135}$ (95% CONFIDENCE LEVEL)

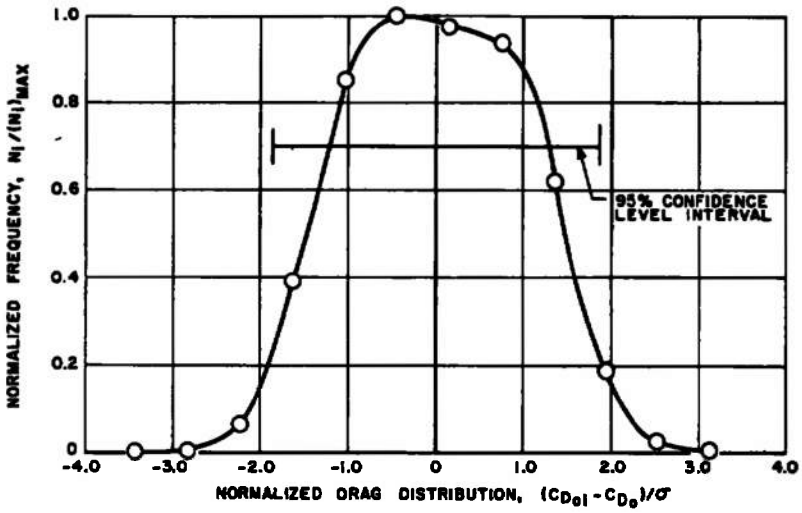

p. Ballute (Config. 17), $M_\infty = 3.67$

Fig. 8 Continued

C_{D_0}	σ	SKEWNESS	KURTOSIS	$(N_i)_{MAX}$	N
0.1359	0.0405	0.6115	3.7256	773	15963

$C_{D_0} = 0.1359 \; {}^{+0.0903}_{-0.0680}$ (95 % CONFIDENCE LEVEL)

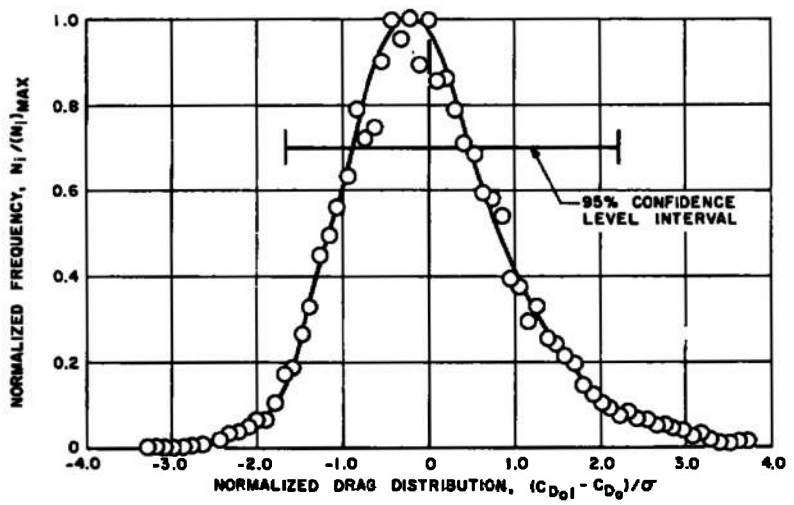

q. Ballute (Config. 5), $M_\infty = 3.67$

C_{D_0}	σ	SKEWNESS	KURTOSIS	$(N_i)_{MAX}$	N
1.1785	0.2272	0.5238	10.586	1789	15864

$C_{D_0} = 1.1785 \; {}^{+0.4612}_{-0.4476}$ (95% CONFIDENCE LEVEL)

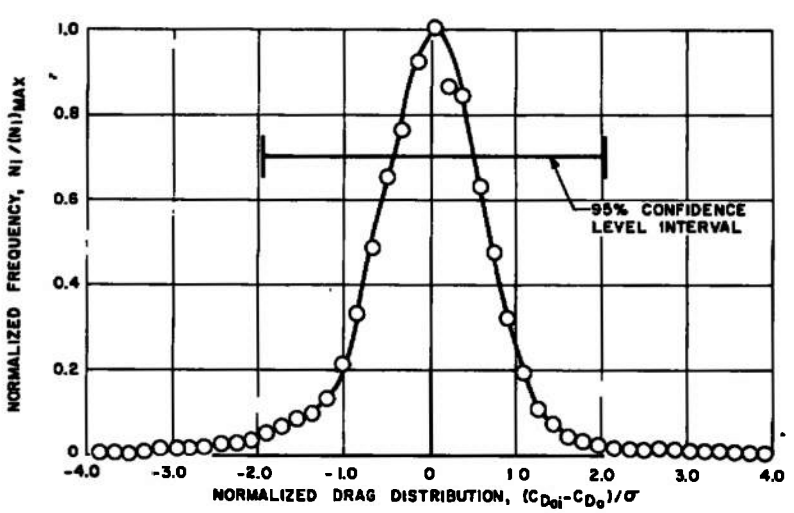

r. Ballute (Config. 18), $M_\infty = 3.68$

Fig. 8 Concluded

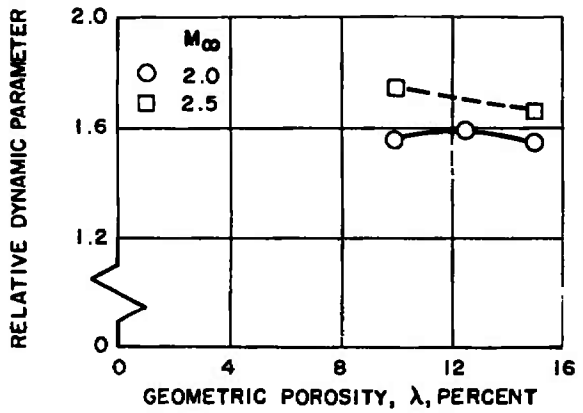

Fig. 9 Variation of Relative Dynamic Parameter with Parachute Geometric Porosity, Aeroshell Not Attached

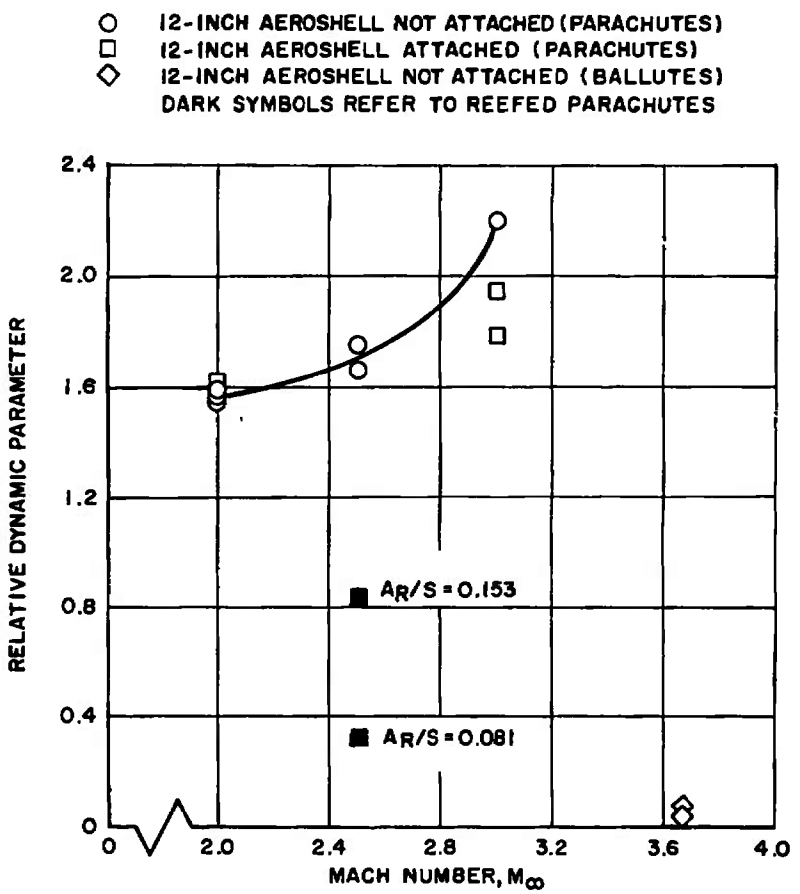

Fig. 10 Variation of Decelerator Relative Dynamic Parameter with Free-Stream Mach Number

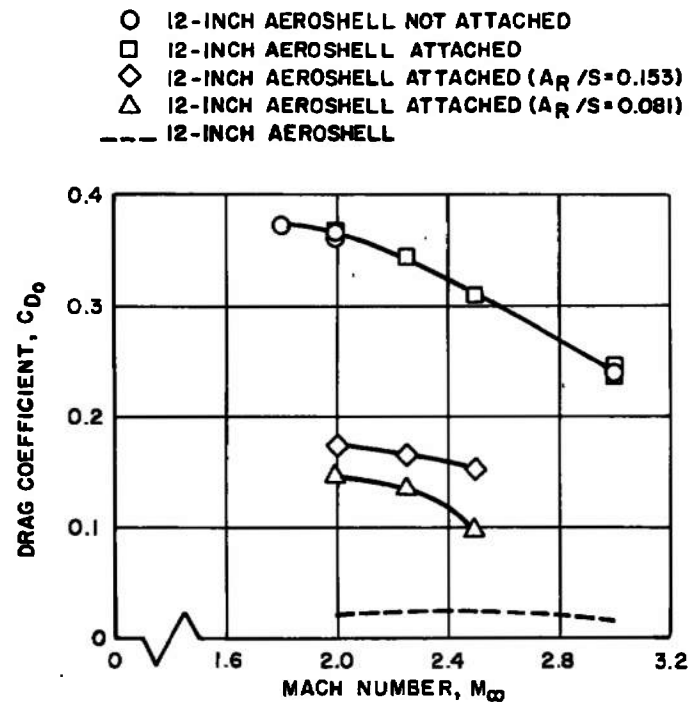

Fig. 11 Variation of Parachute-plus-Forebody Drag Coefficient with Free-Stream Mach Number, DGB 12.5-percent Porosity Parachute

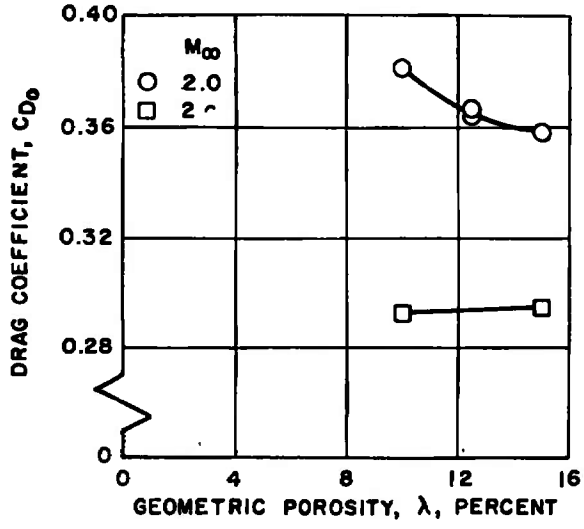

Fig. 12 Variation of Parachute-plus-Forebody Drag Coefficient with Parachute Geometric Porosity, Aeroshell Not Attached

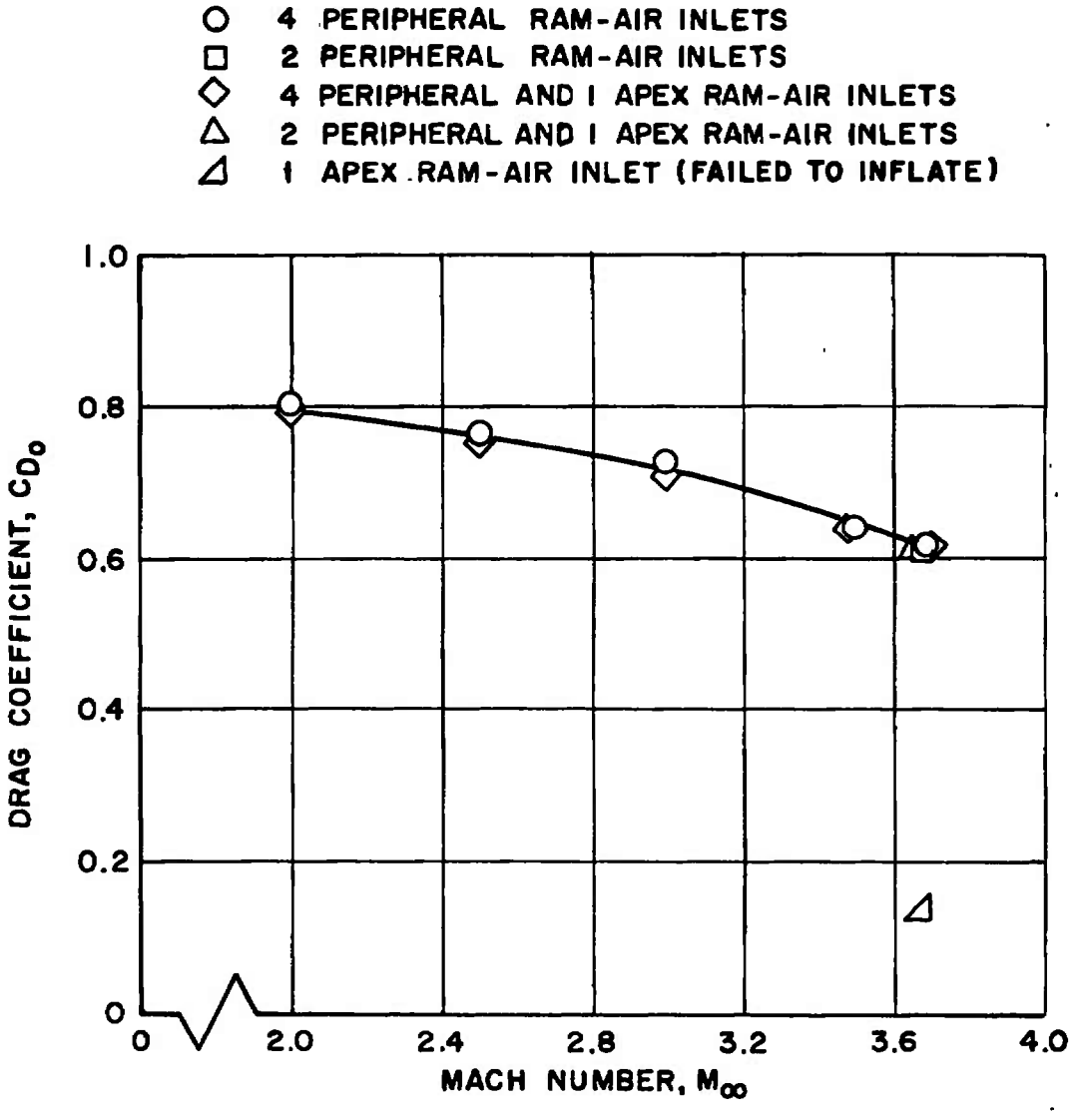

Fig. 13 Variation of Ballute-plus-Forebody Drag Coefficient with Free-Stream Mach Number, Aeroshell Not Attached

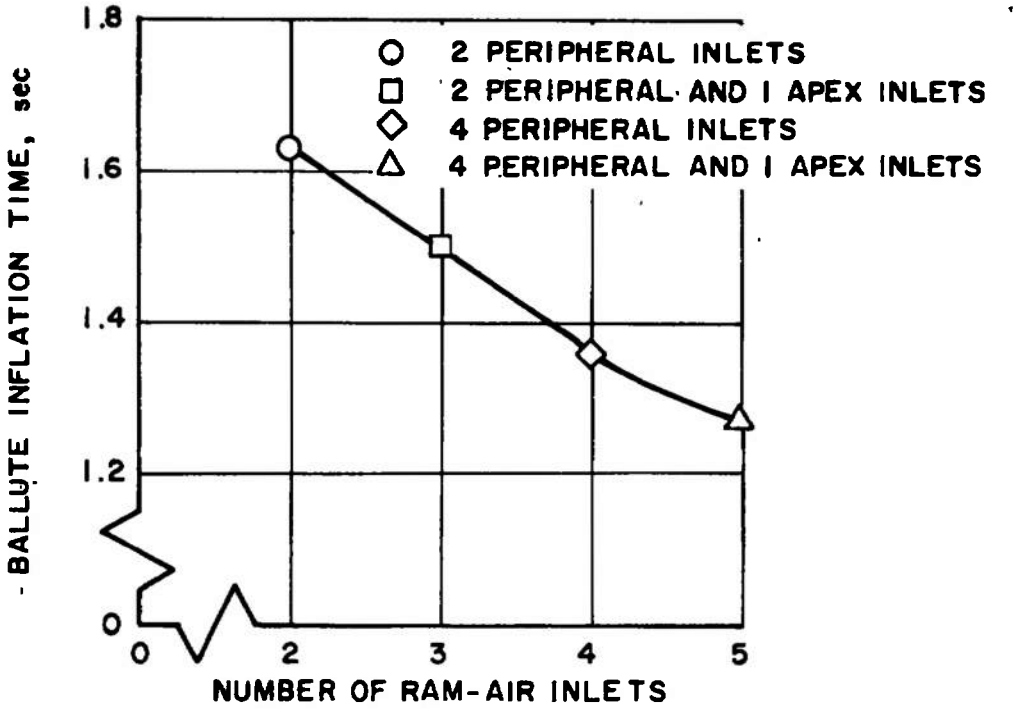

Fig. 14 Effect of Number of Ram-Air Inlets on Ballute Inflation Time, M_∞ = 3.7, Aeroshell Not Attached

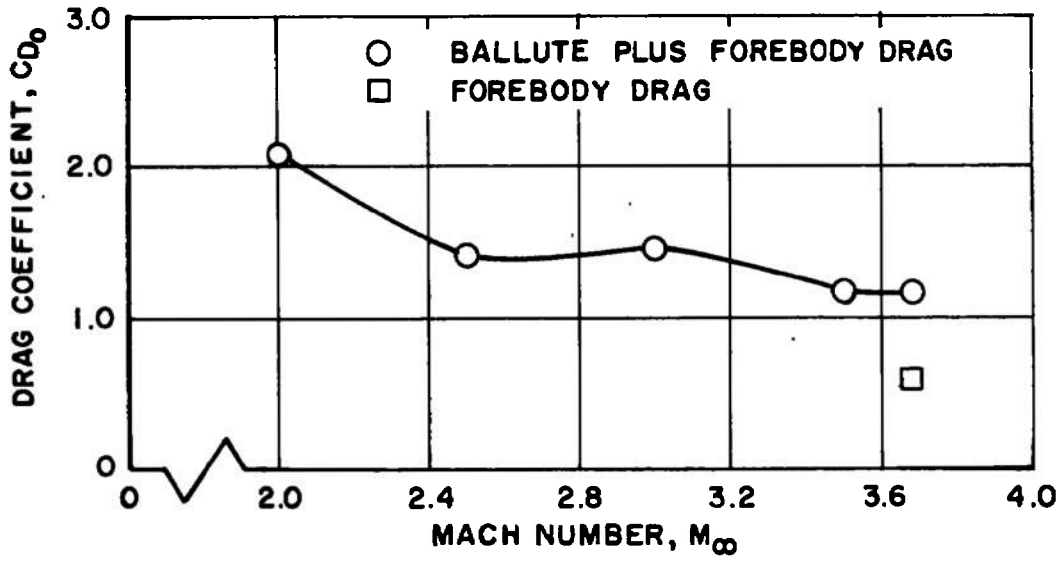

Fig. 15 Variation of Ballute-plus-Forebody Drag Coefficient with Free-Stream Mach Number, 15-in.-Diam Ballute, Attached 19-in.-Diam Aeroshell

APPENDIX II
STATISTICAL ANALYSIS PROGRAM

A statistical program was used to analyze the decelerator dynamic drag data recorded on a high-speed digital data recording system at a sample rate of 1000 samples per second. In general, the statistical program permitted a quantitative evaluation to be made of the dynamic drag characteristics of each decelerator tested during this investigation. The first four "central moments" - average drag coefficient, standard deviation, skewness, and kurtosis - were determined from each group of data samples obtained for each decelerator; and these values were inspected for conformity to a normal (or Gaussian) distribution for the purpose of determining confidence levels. The significance of each central moment (or distribution parameters, as they are referred to in this report) and the computer program used to obtain these parameters are briefly discussed.

DRAG DISTRIBUTION PARAMETERS

Average Drag Coefficient (C_{D_o})

The average value of a finite number of observations is the most probably value of the quantity. Expressed mathematically in terms of drag coefficient,

$$C_{D_o} = \frac{1}{N} \sum_{i=1}^{n} N_i C_{D_{oi}}$$

where

$C_{D_{oi}} = C_{D_{o1}}, C_{D_{o2}}, \ldots . C_{D_{on}}$ = mean drag coefficient value of each cell

$N_i = N_1, N_2, \ldots . N_n$ = number of drag coefficient values stored in each cell

$N = N_1 + N_2 + \ldots . N_n$ = total number of samples

Standard Deviation (σ)

The standard deviation is the rms deviation of the mean drag coefficient value of each cell from the average drag coefficient value. Expressed mathematically,

$$\sigma = \left[\frac{1}{N} \sum_{i=1}^{n} N_i (C_{D_{oi}} - C_{D_o})^2 \right]^{0.5}$$

Skewness ($\sqrt{\beta_1}$)

Skewness is a measure of the asymmetry of a distribution of data. The distribution is said to be positively or negatively skewed depending on whether the distribution extends to the right or left of the average drag coefficient value, respectively. Expressed mathematically and normalized with respect to standard deviation,

$$\sqrt{\beta_1} = \frac{1}{N\sigma^3} \sum_{i=1}^{n} N_i (C_{D_{oi}} - C_{D_o})^3.$$

Kurtosis (β_2)

Kurtosis is a measure of the peakedness of a distribution of data. Expressed mathematically and normalized with respect to standard deviation,

$$\beta_2 = \frac{1}{N\sigma^4} \sum_{i=1}^{n} N_i (C_{D_{oi}} - C_{D_o})^4$$

The average drag coefficient and standard deviation are the most important parameters of a distribution of data, whereas both skewness and kurtosis are indications of how well an actual distribution conforms to a normal distribution. For a normal distribution, skewness is zero and kurtosis has a value of three. If kurtosis for an actual distribution is greater than three, the distribution is more peaked than a normal distribution; and if kurtosis is less than three, the distribution is less peaked than a normal distribution.

The standard deviation for a normal distribution uniquely defines the percentage of all data that fall between specified confidence levels. For example, 68.27, 95.45, and 99.73 percent of all data will fall between $\pm 1\sigma$, $\pm 2\sigma$ and $\pm\sigma$, respectively, if the distribution is a normal distribution. For an actual distribution, use of the Pearson distribution approximation (Ref. 4), which is a function of skewness and kurtosis, permits an evaluation to be made of the percentage of all data that fall between specified confidence levels. For this investigation, the Pearson distribution approximation was used because the distribution of decelerator dynamic drag data did not conform to a normal distribution with sufficient accuracy to justify the use of the confidence levels inherent for a normal distribution.

The most significant portion of the computer program was the procedure followed for grouping the data into a finite number of cells that covered the range of drag coefficient values recorded by the high-speed

digital data recording system. Each cell was assigned a given range of drag coefficient values and a mean drag coefficient value that was the average of that range. All cells were of equal span, and a total of 70 cells with appropriate cell boundaries was adequate for defining the distribution density plots presented in this report. The distribution density plots presented in this report represent the information obtained from approximately 16,000 data samples for each decelerator tested.

TABLE I
DECELERATOR TEST SUMMARY

CONFIGURATION NUMBER	DECELERATOR	MACH NUMBER, M_∞	DYNAMIC PRESSURE q_∞, psf	REENTRY MODEL CONFIGURATION	X/D	INFLATION TIME, SEC	C_{D_o}	RELATIVE DYNAMIC PARAMETER	REEFED AREA RATIO, A_R/S	REMARKS
8	DGB-10%	2.00	69.20	1 *	13.60	0.45	0.3810	1.56	-----	1) Parachute failed during Mach number change
10	DGB-10%	2.50	70.00	1	13.60	0.51	0.2931	1.75	0.054	1) Disreefed 3 sec after deployment 2) Parachute failed during Mach number change
7	DGB-12.5%	2.00	69.80	1	13.60	0.44	0.3670	1.59	-----	1) Parachute failed during Mach number change
15	DGB-12.5%	2.00	70.00	1	13.60	0.62	0.3636	1.13	0.146	1) Disreefed 3 sec after deployment
15	DGB-12.5%	1.80	69.30	1	13.60	----	0.3722	----	-----	
6	DGB-12.5%	3.00	69.90	1	13.60	0.45	0.2383	2.20	-----	1) Parachute failed during Mach number change
3	DGB-12.5%	2.00	70.30	2	6.80	3.00	0.3691	1.62	-----	1) Suspension lines twisted during deployment
3	DGB-12.5%	2.25	69.90	2	6.80	----	0.3452	----	-----	
3	DGB-12.5%	2.50	69.90	2	6.80	----	0.3103	----	-----	2) Parachute failed during Mach number change
19	DGB-12.5%	2.50	70.00	2	6.80	0.56	0.1534	0.93	0.152	
19	DGB-12.5%	2.23	60.50	2	6.80	----	0.1858	----	0.153	
19	DGB-12.5%	2.00	70.20	2	6.80	----	0.1748	----	0.153	
20	DGB-12.5%	2.50	70.10	2	6.80	0.53	0.0991	0.32	0.081	
20	DGB-12.5%	2.25	69.90	2	6.80	----	0.1368	----	0.081	
20	DGB-12.5%	2.00	70.30	2	6.80	----	0.1497	----	0.081	
1	DGB-12.5%	3.00	70.20	2	6.80	0.54	0.2482	1.94	-----	1) Parachute failed during Mach number change
2	DGB-12.5%	3.00	69.90	2	8.80	0.58	0.2388	1.78	0.338	1) Disreefed 3 sec after deployment 2) Parachute failed during Mach number change
9	DGB-15%	2.00	68.90	1	13.60	0.42	0.3587	1.55	----	1) Parachute failed during Mach number change
11	DGB-15%	2.50	70.20	1	13.60	0.44	0.2953	1.68	0.081	1) Disreefed 10 sec after deployment 2) Parachute failed during Mach number change

* 1. Aeroshell not attached

2. Attached 12-in.-diam aeroshell

3. Attached 19-in.-diam aeroshell

TABLE I (Concluded)

CONFIGURATION NUMBER	DECELERATOR	MACH NUMBER, M_∞	DYNAMIC PRESSURE, q_∞, psf	REENTRY MODEL CONFIGURATION	X/D	INFLATION TIME, SEC.	C_{D_o}	RELATIVE DYNAMIC PARAMETER	REMARKS
4	Ballute	3.68	70.20	1	7.61	1.63	0.6182	0.08	1) Same as Configuration 13 except two peripheral located ram-air inlets are closed off
13	Ballute	3.69	70.10	1	7.01	1.36	0.6218	0.05	1) Four peripheral located ram-air inlets
13	Ballute	3.51	70.50	1	7.01	----	0.6454	----	2) 4-ft-diam ballute
13	Ballute	3.01	69 80	1	7.01	----	0.7308	----	
13	Ballute	2 50	70.30	1	7.01	----	0.7685	----	
13	Ballute	2.00	70.8	1	7.01	----	0.8074	----	
12	Ballute	3 69	70.00	1	7.57	1.27	0.6168	0.05	1) Four peripheral located ram-air inlets and one apex located ram-air inlet
12	Ballute	3.51	71.00	1	7.57	-----	0.6470	----	2) 4-ft-diam ballute
12	Ballute	3.01	70.00	1	7.57	----	0.7080	----	
12	Ballute	2.50	70.10	1	7.57	----	0.7570	----	
12	Ballute	2.00	70.00	1	7.57	----	0.7915	----	
17	Ballute	3 67	70.40	1	7.57	1.50	0.6142	0.04	1) Same as Configuration 12 except two peripheral located ram-air inlets are closed off
5	Ballute	3.67	70.60	1	7.57	----	0.1359	1.17	1) Ballute did not inflate 2) Same as Configuration 12 except all peripheral ram-air inlets are closed off
18	Ballute	3.68	70.30	3	4.00	0.90	1.1785	0.77	1) Four peripheral located ram-air inlets
18	Ballute	3 50	71.80	3	4.00	----	1.1784	----	2) 15-in.-diam ballute
18	Ballute	3.00	69.80	3	4.00	----	1.4524	----	
18	Ballute	2.50	70.00	3	4.00	----	1.4053	----	
18	Ballute	2 00	70 00	3	4.00	----	2.0783	----	

UNCLASSIFIED

Security Classification

DOCUMENT CONTROL DATA - R & D

(Security classification of title, body of abstract and indexing annotation must be entered when the overall report is classified)

1. ORIGINATING ACTIVITY (Corporate author)	2a. REPORT SECURITY CLASSIFICATION
Arnold Engineering Development Center ARO, Inc., Operating Contractor Arnold Air Force Station, Tennessee	UNCLASSIFIED
	2b. GROUP N/A

3 REPORT TITLE

AERODYNAMIC CHARACTERISTICS OF BALLUTES AND DISK-GAP-BAND PARACHUTES AT MACH NUMBERS FROM 1.8 TO 3.7

4. DESCRIPTIVE NOTES (Type of report and inclusive dates)

July 30 to September 13, 1969 - Final Report

5. AUTHOR(S) (First name, middle initial, last name)

Lawrence L. Galigher, ARO, Inc.

6. REPORT DATE	7a. TOTAL NO. OF PAGES	7b. NO. OF REFS
November 1969	44	4

8a. CONTRACT OR GRANT NO.	9a. ORIGINATOR'S REPORT NUMBER(S)
F40600-69-C-0001	
b. PROJECT NO. 6065	AEDC-TR-69-245
c. Program Element 62201F	9b. OTHER REPORT NO(S) (Any other numbers that may be assigned this report) N/A
d.	

10. DISTRIBUTION STATEMENT This document is subject to special export controls and each transmittal to foreign governments or foreign nationals may be made only with prior approval of Air Force Flight Dynamics Laboratory (FDFR), Wright-Patterson AF Base, Ohio 45433.

11. SUPPLEMENTARY NOTES	12. SPONSORING MILITARY ACTIVITY
Available in DDC	Air Force Flight Dynamics Laboratory Air Force Systems Command Wright-Patterson AF Base, Ohio 45433

13. ABSTRACT

A test was conducted in Propulsion Wind Tunnel, Supersonic (16S) to determine deployment characteristics and aerodynamic performance of disk-gap-band parachutes of various geometric porosities and ballutes with various ram-air inlet configurations. Deployments were made from a reentry-type model at nominal free-stream Mach numbers from 2.0 to 3.7 at a nominal free-stream dynamic pressure of 70 psf. Eight of the twelve parachutes tested failed shortly after data acquisition at the deployment Mach number test conditions. The six ballutes tested retained their structural integrity throughout the range of Mach numbers investigated.

This document is subject to special export controls and each transmittal to foreign governments or foreign nationals may be made only with prior approval of Air Force Flight Dynamics Laboratory (FDFR), Wright-Patterson AF Base, Ohio 45433.

DD FORM 1 NOV 65 1473

UNCLASSIFIED

Security Classification

UNCLASSIFIED
Security Classification

14. KEY WORDS	LINK A		LINK B		LINK C	
	ROLE	WT	ROLE	WT	ROLE	WT
aerodynamic characteristics						
deployment						
1. parachutes --						
deceleration						
supersonic wind tunnels						
2. Ballutes						
3 Disk gap band parachutes						
1-15.						

AFSC
Arnold AFS Tenn

UNCLASSIFIED
Security Classification